Title

Tracking transient changes in the intrinsic neural frequency architecture: Oxytocin facilitates non-harmonic relationships between alpha and theta rhythms in the resting brain

Running Title:

Oxytocin induces alpha:theta non-harmonicity

Authors and affiliations

Kaat Alaerts[1#], Aymara Taillieu[1], Jellina Prinsen[1], Nicky Daniels[1]

[1]KU Leuven, Department of Rehabilitation Sciences, Research Group for Neurorehabilitation, Tervuursevest 101 box 1501, 3001 Leuven, Belgium.

[#] **Corresponding author:**

Kaat Alaerts

KU Leuven, Department of Rehabilitation Sciences, Research Group for Neurorehabilitation, Tervuursevest 101 box 1501, 3001 Leuven, Belgium.

E-mail: kaat.alaerts@kuleuven.be

Tel.: +32 16 37 64 46, Fax: +32 16 32 91 97

Figures	5
Supplementary Information	
Supplementary Figure	1

Key words

oxytocin, electroencephalography, cross-frequency, alpha, theta, heart rate variability

Abstract

Shifts in the peak frequencies of oscillatory neural rhythms have been put forward as a principal mechanism by which cross-frequency coupling and decoupling is implemented in the brain. This notion is based on the mathematical reality that neural oscillations can only fully synchronize when their peak frequencies form harmonic 2:1 relationships (e.g., $f_2=f_1/2$). Non-harmonic cross-frequency relationships, on the other hand (based on the irrational golden mean 1.618..:1), provide the highest physiologically possible desynchronized state (reducing the occurrence of spurious, noisy, background coupling), and are therefore anticipated to characterize the resting state of the brain, in which no selective information processing takes place.

The present study sought to assess whether the transient occurrence of 1.6:1 non-harmonic and 2:1 harmonic relationships between peak frequencies in the alpha (8–14 Hz) and theta (4–8 Hz) bands - respectively facilitating states of decoupling or coupling between oscillatory rhythms - are impacted by the intranasal administration of a single-dose of oxytocin (OT) or placebo. To do so, continuous resting-state electroencephalography (5 min eyes open, 19 electrodes) was obtained from 96 healthy adult men before and after nasal spray administration.

The transient formation of non-harmonic cross-frequency configurations between alpha and theta peak frequencies was significantly increased after OT nasal spray administration, indicating an effect of OT on reducing the intrinsic occurrence of spurious (noisy) background phase synchronizations during resting-state. As a group, the OT group also showed a significant parallel increase in high-frequency and decrease in low-frequency heart rate variability, confirming a homeostatic role of OT in balancing parasympathetic drive.

Overall, non-harmonic cross-frequency configurations have been put forward to lay the ground for a healthy neural network allowing the opportunity for an efficient transition from resting state to activity. The observed effects of OT on cross-frequency dynamics are therefore interpreted to reflect a homeostatic role of OT in increasing the signal-to-noise properties of the intrinsic EEG neural frequency architecture, i.e., by precluding the occurrence of ‘noisy’, unwanted, spurious couplings among neural rhythms in the resting brain.

Introduction

In recent years, there has been a growing interest in studying the psychobiological systems that underlie homeostasis and stress regulation. One neurobiological system that is suggested to play a pivotal role in these regulatory processes is the oxytocinergic system with its wide-spread expression of receptors both centrally at the level of the brain, as well as in peripheral tissues (e.g. heart). The neuropeptide oxytocin (OT) is produced in the hypothalamus from where neurons in the paraventricular nuclei (PVN) have direct projections to distinct (social) brain structures in the limbic system (e.g. amygdala), the reward system and the frontal and temporal lobes (Wigton et al., 2015). As a neuromodulator, OT is linked to a range of complex (social) behaviors, including social reciprocity, attunement and social attachment (Bartz et al., 2011), but the exact neural substrates underlying OT's neuromodulatory function remain not fully understood. On the one hand, theoretical accounts suggest a role of OT in top-down modulation of social salience, enhancing social sensitivity (Shamay-Tsoory and Abu-Akel, 2016), while on the other hand, OT is implicated in exerting a bottom-up function in regulating central and autonomic homeostatic function impacting (social) stress and anxiety responses (Stoop, 2012).

Human neuroimaging studies into the neural effects of OT have predominantly employed functional magnetic resonance imaging, demonstrating changes in brain function and connectivity within wide-spread subcortical-cortical neural networks with high spatial precision (Wigton et al., 2015). Only few studies have examined the effects of OT on neural processing in the temporal domain by using electroencephalography (EEG) neuroimaging methods with high temporal resolution for assessing OT-induced changes in e.g., event-related potentials (de Bruijn et al., 2017; Peltola et al., 2018; Ruissen and de Bruijn, 2015; Waller et al., 2015; Ye et al., 2017) and EEG band power activity (Festante et al., 2020; Rutherford et al., 2018; Singh et al., 2016; Soriano et al., 2020; Wynn et al., 2019).

Ever since the advent of EEG recordings at the human scalp, neuronal populations that reside in the brain have been consistently shown to fire at discrete frequency bands (e.g., delta, theta, alpha, beta bands). It is generally assumed that the entrainment of oscillatory activity to these particular rhythms provides the basic mechanism by which information transfer is accomplished within and across neuronal cell populations (Fries, 2005). While low frequency rhythms are hypothesized to

originate from large-scale (whole-brain) networks, high frequency activity is thought to reflect more local processing phenomena (Varela et al., 2001). Furthermore, synchronization of neural oscillations in different frequency bands ('cross-frequency coupling') is proposed to form the core mechanism for the coordination and integration of neural systems at different spatio-temporal scales (Roopun et al., 2008; Sauseng et al., 2008).

Mathematically, two oscillators of different frequencies can only fully synchronize when forming harmonics ($f_2 = f_1/2$; e.g. f_1 = 10 Hz and f_2 = 5 Hz), i.e., allowing a pattern of frequent and regular excitatory phase meetings (cross-frequency coupling). Non-harmonic relationships between two oscillators, on the other hand, will prevent irregular phase meetings. Mathematically, it was shown that two rhythms will *never* spontaneously synchronize when their ratio approximates the golden mean ratio 1.618...:1, i.e. constituting the most irrational ratio between two rhythms ($f_2 = f_1/1.6$; e.g. f_1 = 10 Hz and f_2 = 6.18 Hz) (Pletzer et al., 2010).

Based on this mathematical reality, a theoretical framework was posited by Klimesch et al. (Klimesch, 2012, 2013, 2018; Rassi et al., 2019), hypothesizing that the specific frequency architecture of neural oscillations may approximate a geometrical series of exponent 2 (e.g. δ = 2.5, θ = 5, α = 10, β = 20, γ = 40, etc…) to entail optimal frequency domains for facilitating cross-frequency coupling (i.e., based on harmonic numerical ratios), as well as for facilitating controlled cross-frequency decoupling (i.e., based on non-harmonic numerical ratios approximating the golden mean 1.618…). Accordingly, transient changes in the peak frequency of different rhythms are proposed to form a flexible mechanism to maximize cross-frequency coupling or decoupling with neighboring frequency domains (Klimesch, 2012). For example, the specific arrangement of the peak frequencies of two adjacent frequency bands (e.g., alpha and theta) will determine whether they will form a harmonic (e.g.10/5 Hz = ratio 2:1) or non-harmonic relationship (e.g., 10/6.18 Hz = ratio 1.6:1) and, consequently, whether their synchronization will be facilitated or prevented. In line with this hypothesis, recent research has shown state- and task-dependent shifts in peak frequencies to be associated with transient shifts in harmonic/non-harmonic cross-frequency dynamics (Rodriguez-Larios and Alaerts, 2019, 2020; Rodriguez-Larios et al., 2020a; Rodriguez-Larios et al., 2020b). For example, the occurrence of harmonic cross-frequency arrangements (2:1) between theta and alpha rhythms - both implicated in executive control and working memory - was shown to be most prominent during active cognitive processing, whereas the formation of non-harmonic arrangements (1.6:1) were more

prominent during rest and a non-cognitively demanding breath focus meditation, both in novices (Rodriguez-Larios and Alaerts, 2019, 2020) and experienced mediators (Rodriguez-Larios et al., 2020a). Also longitudinally, pre-to-post increases in the occurrence of non-harmonic cross-frequency arrangements (1.6:1) were observed after an 8-week mindfulness training course (Rodriguez-Larios et al., 2020b), together indicating that meditative practice facilitated a preclusion of unwanted 'spurious' interactions among theta and alpha neural rhythms, implicated in executive and memory processes.

Indeed, especially during resting or meditative states, the brain's intrinsic neural circuitry may adjust its frequency architecture to a state in which cross-frequency decoupling is actively facilitated to avoid spurious (unwanted) phase synchronization (at non-harmonic ratio 1.6:1) (Pletzer et al., 2010). During active cognitive task demands, on the other hand, the brain's neural circuitry may inversely adjust its frequency architecture to a state in which cross-frequency coupling (harmonic ratio 2:1) is facilitated, allowing enhanced information transfer for neural processing (Klimesch, 2013; Pletzer et al., 2010). Notably, previous research showed a proportionally high incidence of alpha:theta cross-frequency relationships approximating the non-harmonic 'decoupled' 1.6:1 cross-frequency state (particularly during rest), providing experimental support that this configuration forms a prevalent intrinsic physiological state (Rodriguez-Larios and Alaerts, 2019, 2020). In a mathematical sense, the golden mean cross-frequency relationship provides the highest physiologically possible desynchronized state and is therefore anticipated to characterize the resting state of the brain, in which no selective information processing takes place (Pletzer et al., 2010). Its configuration is hypothesized to lay the ground for a healthy neural network allowing the opportunity for an efficient transition from resting state to activity (Pletzer et al., 2010). In this view, preventing 'noisy', spurious background couplings may form an important mechanism for enhancing signal-to-noise properties of the neural network, optimally preparing the system for forthcoming active signal processing states.

At the neuronal level, Owen et al. (2013) recently put forward an influential overarching mechanism by which OT may exert its wide range of neuromodulatory effects, showing that OT enhances signal-to-noise ratio properties of synaptic transmissions in mammalian hippocampal tissue by suppressing spontaneous (noisy) neuronal firings thereby enhancing the fidelity of spike transmission (Owen et al., 2013). Later work showed that these cellular mechanisms translate to network oscillatory patterns, demonstrating an impact of OT on suppressing sharp wave-ripple complexes while at the same time increasing the temporal precision of oscillation-coupled spikes in

mouse hippocampal tissue (Maier et al., 2016). Also in vivo rodent research demonstrated OT receptor activity of olfactory bulb neurons to increase peak firing responses to social sensory information (odorants) by lowering their (spontaneous) baseline firing, hence augmenting signal-to-noise properties for signal transmission (Oettl et al., 2016). Together, these prior studies suggest that the induction of high signal-to-noise states may form a shared over-arching mechanism by which OT may amplify signal value of neuronal processes within wide-spread neural circuits, i.e., by reducing 'noise' (Owen et al., 2013).

Here, we took advantage of the high temporal resolution of EEG to examine a potential role of OT in modulating signal-to-noise properties at the brain's system's level, i.e., by assessing variations in intrinsic EEG cross-frequency dynamics between alpha and theta oscillatory rhythms and the extent of spurious 'noisy' background phase synchronizations during resting-state. Within a randomized, placebo-controlled design, continuous resting-state EEG (5 min, eyes open, 19 electrodes) was obtained from healthy adult men before and after administration of a single-dose of OT or placebo (PL) nasal spray to assess whether OT impacts the transient formation of non-harmonic or harmonic cross-frequency relationships between alpha and theta peak frequencies, respectively facilitating a state of decoupling or coupling between oscillatory rhythms. In line with prior reports of OT's effect on signal-to-noise properties (Owen et al., 2013), intranasal OT administration is primarily hypothesized to facilitate the brain's intrinsic neural frequency architecture into a 'decoupled' state (i.e., increased transient occurrence of non-harmonic 1.6:1 alpha:theta cross-frequency relationships), thereby avoiding spurious (noisy) background phase synchronizations during resting-state, hence enhancing system-level signal-to-noise properties.

As an additional outcome, effects of OT on resting-state heart rate variability (HRV) were also obtained to examine whether OT's effects on EEG cross-frequency dynamics are paralleled by changes in high- and/or low-frequency HRV (both established markers of autonomic nervous system (ANS) activity). These examinations will allow exploring how OT's neural effects on intrinsic coupling/decoupling relate to prior observations of a homeostatic role of OT in terms of enhancing intrinsic ANS parasympathetic tone (i.e., OT-induced increases in high-frequency HRV) (Jain et al., 2017; Kemp et al., 2012; Martins et al., 2020; Norman et al., 2011).

Methods

Participants

Subjects were recruited to participate in a single lab-session during which neurophysiological recordings were performed before and after nasal spray administration of oxytocin (OT) or placebo (PL). Rest EEG recordings were completed by a total of 102 (male) participants of which 53 received the OT nasal spray (mean age 22.37 ± 3.12 years) and 49 received the PL nasal spray (mean age 22.50 ± 3.00 years). Due to excessive signal artifacts, EEG data were not available for a subset of participants (4 OT and 2 PL), and therefore final analyses were conducted for a total of 96 participants (49 OT, 47 PL) (see CONSORT Flow diagram). All participants abstained from alcohol and caffeine 24 hours before testing. Written informed consent was obtained from all participants prior to the study. Inclusion criteria for participation were: male; aged between 18-35 years; right-handed; and corrected-to-normal vision. Further, since information sheets and consent forms were only available in Dutch, only native-Dutch speaking participants were included. Exclusion criteria encompassed any self-reported usage of psychotropic medication or known neurological or psychiatric condition. Consent forms and study design were approved by the Ethics Committee Research UZ/KU Leuven in accordance with The Code of Ethics of the World Medical Association (Declaration of Helsinki). The recordings of rest EEG were part of larger assessment protocols (registered at ClinicalTrials.gov NCT03272321 and NCT04443647), assessing the effect of OT on stress neurophysiology (e.g., skin conductance) (Daniels et al., 2020; Soriano et al., 2020).

Nasal spray administration

Participants were randomly assigned to receive a single-dose of OT or PL based on a computer-generated randomized order. Except for the manager of randomization and masking of drug administration, all participants and research-staff conducting the study were blind to treatment allocation. In correspondence with previous studies (Guastella and MacLeod, 2012), participants received 24 international units (IU) of OT (Syntocinon®, Sigma-tau) or PL containing a saline (natrium-chloride) solution. Participants received 3 puffs per nostril in an alternating fashion with each puff containing 4 IU. For inhalation of the spray, participants were instructed to take a deep breath through the nose and to tilt their head slightly backwards during nasal administration in order to minimize gravitational loss of the spray (according to recommendations for standardized use (Guastella et al.,

2013)). In healthy humans, the impact of OT on social cognition is commonly evaluated using a 30–45 min wait-time before initiation of the experimental task (see (Guastella and MacLeod, 2012)). Accordingly, in the current study, a 30-min wait-time was incorporated prior to initiating the post-session recording in order to assess the effects of intranasal OT during peak OT-concentrations.

EEG recordings and preprocessing

Recording. Rest EEG recordings (5 min session) were performed before and 30 min after nasal spray administration. During the recordings, the participants were instructed to relax, to avoid excessive movements and to fixate on a cross presented in front of them. The Nexus-32 multimodal acquisition system and BioTrace+ software (version 2015a, Mind Media, The Netherlands) were used to collect continuous EEG recordings with a 21-electrode cap (MediFactory, The Netherlands) positioned according to the 10–20 system. Skin abrasion and electrode paste (Nuprep) were used to reduce electrode impedance. The sampling rate for the digitized EEG-signal was 256 Hz.

Preprocessing. Preprocessing was performed through custom MATLAB scripts and EEGlab functions (MATLAB version r2020b). After removal of the first three sec of the recording, raw EEG data were filtered with the *eegfiltnew* function using Hamming windowed sinc FIR high- (0.5 Hz) and low-pass filters (40 Hz). Flat channels were detected and removed (*clean_flatlines*) and the artifact subspace reconstruction function (*clean_asr*) was conducted to remove residual artifactual signal. Noisy channels were interpolated. The remaining epochs were then concatenated and the continuous signals were mathematically re-referenced offline to linked ears (average of A1 and A2).

Transient peak detection and determination of cross-frequency relationships

The time-frequency representation of the EEG data was obtained using short-term Fast Fourier Transform (STFFT) computed through MATLAB *spectrogram* function (Hanning window length of 1 sec and sliding step of 25 bins; i.e. 90.23 % overlap), with a frequency precision of 10 points per frequency (i.e. from 0.1 Hz until 40 Hz in 400 frequency lines). Then, transient peak frequencies of the theta (4–8 Hz) and alpha (8–14 Hz) bands were detected for each (overlapping) 1 sec epoch of transformed data using the find local maxima function implemented in MATLAB r2020b (i.e. *findpeaks*) (similar to procedures described in (Rodriguez-Larios and Alaerts, 2019)). With this algorithm, data samples that are larger than their two neighboring samples were identified as ‘local peaks’ within the

specified alpha and theta frequency ranges. For a limited number of epochs (5.19 % of total number of epochs, across electrodes and participants), no clear peaks were detected in the theta or alpha bands and these epochs were therefore excluded from further analyses. When two or more peaks were detected in one frequency band, only the peak with highest amplitude was selected. Based on the identified peak frequencies, the numerical ratio of the alpha and theta peaks (peak-frequency$_{alpha}$/ peak-frequency$_{theta}$) was calculated for each epoch and rounded to the first decimal place (e.g., 10/5 Hz = 2.0). Hence, the obtained ratio-values ranged between 1.1 and 3.4 in steps of 0.1.

Finally, the proportion of epochs in which the alpha:theta peak ratio equaled 1.6 or 2.0 (henceforward termed non-harmonic 'decoupling' and harmonic 'coupling') was determined for each electrode and participant. **Figure 1A** visualizes the transient (epoch-wise) variability of alpha and theta peak frequencies over time (i.e. 10 sec) for an exemplary subject and electrode, as well as the transient numerical ratio over time. **Figure 1B** visualizes the FFT frequency spectra of two exemplary epochs in which the identified alpha and theta peak frequencies formed a 'harmonic' (2:1) versus a 'non-harmonic' (1.6:1) cross-frequency relationship (partly adapted from (Rodriguez-Larios and Alaerts, 2019)). **Figure 1C** visualizes the distribution of the percentage occurrence of all possible ratios, as recorded at baseline (before nasal spray administration). In line with Rodriguez et al. (2019, 2020), the distribution showed a maximal occurrence of the non-harmonic 1.6:1 alpha:theta ratio aspect (10.16%, average across electrodes), indicating that this configuration forms a highly prevalent physiological state within the intrinsic EEG frequency architecture. The harmonic 2:1 ratio aspect showed an average occurrence of 7.76% (across electrodes).

EEG Statistical analysis

To examine treatment-related changes in the proportion of epochs that displayed 1.6:1 non-harmonic *decoupling* and 2:1 harmonic *coupling*, standardized pre-to-post change scores were calculated for each ratio and subjected to a full repeated-measures ANOVA with the between-subject factor 'treatment' (OT, PL) and the within-subject factors 'cross-frequency ratio' (1.6:1, 2:1) and 'electrode' (19 electrodes).

Subsequently, treatment-related effects were examined separately for the 1.6:1 non-harmonic and 2:1 harmonic ratio aspects, by subjecting pre-to-post changes scores of the OT and PL group to single-sample t-tests (FDR (false-discovery-rate) corrected for multiple comparisons across electrodes). For

each cross-frequency ratio, clusters of electrodes inducing a significant change were adopted in subsequent analyses examining treatment-specificity, i.e., by subjecting pre-to-post change scores to a repeated-measures analysis of variance (ANOVA) with the between-subject factor 'treatment' (OT, PL) and the within-subject factor 'electrode clusters'. All statistics were executed with Statistica version 13 (TIBCO Software Inc., USA).

Heart rate variability recordings and data handling

Photoplethysmography (PPG) recordings were performed simultaneous to the rest EEG (5 min session) using the Nexus-32 multimodal acquisition system at a sampling rate of 128 Hz. The PPG pulse oximeter sensor was placed over the ring finger of the left (non-dominant) hand to monitor blood volume changes in the microvascular bed of the underlying tissue. The time intervals between blood volume pulse waves were assessed using BioTrace32 software (Mind Media, The Netherlands) to derive continuous inter-beat-intervals (IBI) for assessing heart rate variability (HRV). Usability and accuracy of pulse rate variability as an estimate of HRV has been intensively studied and deemed accurate within healthy young subjects at rest (i.e., very good to excellent correspondence between PPG-derived and electrocardiography-derived HRV) (Georgiou et al., 2018; Schäfer and Vagedes, 2013). HRV frequency domain analyses were performed using Kubios HRV Premium software (professional version 3.2) (Tarvainen et al., 2014). All IBI time series were manually inspected prior to analysis and automatic artifact removal, as implemented in Kubios HRV, was performed. A subset of participants was not included in the final analyses due to technical problems with the PPG sensor (7 OT, 3 PL). Of the remaining participants, overall data quality was high (<1% rejected artifacts), consistent with resting-state recording conditions. For each subject and session (pre and post), HRV frequency domain analyses were performed using Fast Fourier Transformation (FFT) based Welch's periodogram to compute the high-frequency (0.15–0.4 Hz) and low-frequency (0.04–0.15 Hz) band power (% relative power) using the power spectral density of the detrended IBI series. Similar to the EEG analyses, ANOVA analyses were conducted to assess treatment-related effects. Treatment-related changes in resting heart rate (average over 5 min session, in beats per minute: bpm) were also assessed using an independent-samples t-test.

Secondary EEG analyses

Treatment-related changes in alpha and theta peak frequencies. In the primary analyses, treatment-related differences in the occurrence of 1.6:1 and 2:1 ratio aspects were assessed. Secondary analyses were performed to explore whether similar treatment-related differences are evident when mean alpha and theta peak frequencies are analyzed separately. Mean peak frequencies of the alpha (8–14 Hz) and theta band (4–8 Hz) were estimated per subject, electrode, and session (pre and post) by averaging the peak frequency of transiently detected peaks over time.

Treatment-related changes in alpha and theta power amplitude estimations. Secondary analyses were performed to explore whether estimations of alpha and theta power amplitudes showed treatment-related changes. After obtaining the time-frequency representation through the MATLAB *spectrogram* function (window length of 1 sec; 90.23 % overlap, 0.1 Hz resolution between 1 and 30 Hz), relative amplitudes (% of overall power, in µV) of the alpha (8–14 Hz) and theta band (4–8 Hz) were estimated per subject, electrode, and session (pre and post).

Finally, additional secondary analyses are reported in **Supplementary Methods** and **Results**, assessing the specificity of the 1.6:1 and 2:1 cross-frequency ratios for inducing treatment-related differences (**Supplementary Figure 1**).

Results

Treatment-related changes in 1.6:1 non-harmonic decoupling and 2:1 harmonic coupling

Full repeated-measures ANOVA analyses of pre-to-post change scores assessing differential treatment effects for the 1.6:1 and 2:1 non-harmonic and harmonic ratios - with the between-subject factor 'treatment' (OT, PL) and the within-subject factors 'cross-frequency ratio' (1.6:1, 2:1) and 'electrode' (19 electrodes) - yielded a significant main effect of 'cross-frequency ratio' ($F(1,94) = 31.59$; $p < .0001$), indicating that across electrodes, participants displayed a general pre-to-post *increase* in the 1.6:1 ratio aspect and a relative *decrease* in the occurrence of 2:1 ratios. However, this main effect needs to be interpreted in light of the significant 'treatment x cross-frequency ratio' interaction effect ($F(1,94) = 5.96$; $p = .017$; $\eta^2 = 0.06$, medium-sized effect), indicating that across electrodes, the differential pre-to-post change in 1.6:1 and 2:1 ratio aspects was significantly more pronounced in the OT group (effect of ratio: ($F(1,94) = 33.18$; $p < .0001$) compared to the PL group (effect of ratio: ($F(1,94) = 4.95$; $p = .028$) (**Figure 2**). None of the other main or interaction effects reached significance (all $p > .05$).

In the next section, treatment-related differences are discussed separately for the 1.6:1 non-harmonic and 2:1 harmonic ratio aspects, as visualized in **Figure 3** and **4**, respectively.

Non-harmonic decoupling (1.6:1 ratio). In the OT group, a large cluster of electrodes (including Fp1, Fp2, F7, F3, Fz, F4, T3, C3, C4, T4, T5, Pz, P4, T6) showed a significant pre-to-post *increase* in the occurrence of the 1.6:1 non-harmonic ratio aspect, indicative of increased *decoupling* between alpha and theta rhythms after intranasal OT administration (all, $t(48) > 2.30$; $p_{FDR} < .05$; **Figure 3A**). In the PL group, none of the electrodes yielded a significant pre-to-post change at the $p_{FDR} > .05$ corrected threshold. ANOVA analysis with the between-subject factor 'treatment' (OT, PL) and the within-subject factor 'cluster electrode' (Fp1, Fp2, F7, F3, Fz, F4, T3, C3, C4, T4, T5, Pz, P4, T6), yielded a significant main effect of treatment ($F(1,94) = 6.10$; $p = .015$; $\eta^2 = 0.06$, medium-sized effect) (**Figure 3B)**, confirming that the pre-to-post increase in the 1.6:1 ratio aspect was significantly more pronounced in the OT group, compared to the PL group.

Harmonic decoupling (2:1 ratio). In the OT group, a cluster of electrodes (including F7, F3, F4, T5, Pz, T6) showed a significant pre-to-post *decrease* in the occurrence of the 2:1 harmonic ratio aspect indicative of decreased *coupling* between alpha and theta rhythms after intranasal OT administration (all $t(48) > 2.30$; $p_{FDR} < .05$; **Figure 4A**). In the PL group, none of the electrodes yielded a significant pre-to-post change at the $p_{FDR} > .05$ corrected threshold. ANOVA analysis on pre-to-post change scores with the between-subject factor 'treatment' (OT, PL) and the within-subject factor 'cluster electrode' (F7, F3, F4, T5, Pz, T6), yielded a significant main effect of treatment ($F(1,94) = 4.75$; $p = .032$; $\eta^2 = 0.05$, small-to-medium-sized effect; **Figure 4B**), confirming that the pre-to-post decrease in the 2:1 ratio aspect was significantly more pronounced in the OT group, compared to the PL group.

Treatment-related changes in HRV

As an additional outcome, changes in resting-state HRV - an established measure of ANS function - were assessed. Repeated-measures ANOVA on pre-to-post HRV change scores with the between-subject factor 'treatment' (OT, PL) and the within-subject factor 'HRV component' (low-frequency HRV, high-frequency HRV) yielded a significant 'treatment x HRV component' interaction effect ($F(1,90) = 6.45$; $p = .013$), indicating a significant increase in (parasympathetic) high-frequency HRV (OT vs PL: $F(1,90) = 6.55$; $p = .012$), and a significant decrease in low-frequency HRV in the OT, compared to the

PL group (OT vs PL: $F(1,91) = 5.85$; $p = .017$) (**Figure 5A**). No significant treatment-related changes were identified in resting heart rate ($t(90) = -0.58$; $p = .56$; OT: -5.02 ± 4.82 bpm (mean ± SD); PL: -5.64 ± 5.19 bpm).

Relationship between cross-frequency (de)coupling and HRV

Spearman correlation analyses revealed a significant negative relationship between baseline recorded low-frequency HRV and the occurrence of the non-harmonic 1.6:1 ratio aspect (in the identified cluster of 14 electrodes), indicating that individuals with a high extent of cross-frequency decoupling display a comparably lower low-frequency HRV (Spearman $R = -.21$; $t(87) = -2.02$; $p = .046$). A trend-level opposite relationship was evident for high-frequency HRV, indicating higher parasympathetic high-frequency HRV in individuals with a higher extent of the non-harmonic 1.6:1 ratio aspect ($R = -.18$; $t(87) = 1.66$; $p = .10$).

While as a group, participants of the OT group displayed significant changes both in terms of HRV and cross-frequency ratio aspects, correlation analyses revealed no significant relationships between the extent of pre-to-post changes in HRV and the extent of pre-to-post changes in the occurrence of the non-harmonic 1.6:1 ratio aspect ($p > .05$). Also, no relationships were evident between baseline or pre-to-post changes in the occurrence of the harmonic 2:1 ratio aspect and low or high frequency HRV (all, $p > .05$).

Secondary EEG analyses

Treatment-related changes in alpha and theta peak frequencies. Repeated-measures ANOVA analyses on pre-to-post change scores with the between-subject factor ‘treatment’ (OT, PL) and the within-subject factors ‘peak frequency’ (alpha, theta) and ‘electrode’ (19 electrodes) yielded a significant main effect of ‘peak frequency’ ($F(1,94) = 47.20$; $p < .0001$), indicating that across electrodes, participants displayed a general pre-to-post increase in peak theta and a relative decrease in peak alpha frequencies. At trend-level, a ‘treatment x peak frequency’ interaction effect was revealed ($F(1,94) = 3.63$; $p = .060$; $\eta^2 = 0.04$, small-to-medium-sized effect), indicating that, albeit evident in both groups, the differential pre-to-post change in theta and alpha peak frequencies was tentatively more pronounced in the OT group (effect of frequency: ($F(1,94) = 39.33$; $p < .0001$) compared to the PL group (effect of frequency: ($F(1,94) = 12.06$; $p < .001$).

Exploratory Spearman correlation analyses showed that pre-to-post decelerations in alpha peak frequencies were related to an increased formation of 1.6:1 non-harmonic ratio aspects (across electrodes: R = -.20; t(94) = -1.97; p = .05). Pre-to-post accelerations in theta peak frequencies on the other hand, were predominantly related to reduced occurrences of 2:1 harmonic coupling (R = -.60; t(94) = -7.36; p < .0001).

Treatment-related changes in alpha and theta power amplitude. Repeated-measures ANOVA analyses on pre-to-post change scores with the between-subject factor 'treatment' (OT, PL) and the within-subject factors 'power amplitude' (alpha, theta) and 'electrode' (19 electrodes) yielded a significant main effect of 'power amplitude' (F(1,94) = 46.22; p < .0001), but no 'treatment x power amplitude' interaction (F(1,94) = .29; p = .59), indicating that, irrespective of treatment, participants displayed a pre-to-post *decrease* in theta power amplitude and a pre-to-post *increase* in alpha power amplitude. Together, these results show that resting spectral power was unaffected by OT administration relative to PL.

Discussion

The present study sought to assess whether the transient occurrence of 1.6:1 non-harmonic and 2:1 harmonic relationships between peak frequencies in the alpha (8–14 Hz) and theta (4–8 Hz) bands - respectively facilitating a state of decoupling or coupling between oscillatory rhythms - are impacted by the intranasal administration of a single-dose of OT or PL. In line with our hypothesis, we showed that the transient formation of non-harmonic cross-frequency 'decoupling' between alpha and theta peak frequencies was significantly increased after OT nasal spray administration, indicating an effect of OT on reducing the intrinsic occurrence of spurious (noisy) background phase synchronizations during resting-state. Additionally, after nasal spray administration, the OT group, not the PL group, showed a significant parallel increase/ decrease in high/ low-frequency HRV.

As a basic mechanism underlying information transfer within and across neuronal cell populations, neurophysiologic research increasingly acknowledged the importance of studying oscillatory brain activity from a cross-frequency perspective, rather than exploring activity (band power) changes within isolated rhythms. In line with this notion, the here adopted method for assessing cross-frequency dynamics (i.e., based on the calculation of transient numerical ratios between peak frequencies of two brain rhythms) allows quantifying short-lived changes in the neural frequency architecture that mathematically enable cross-frequency coupling or decoupling (Klimesch, 2018; Pletzer et al., 2010). In the theoretical accounts by Klimesch (2012, 2013) and Pletzer et al. (2010), the EEG frequency architecture is proposed to entail 'optimal' frequency domains for facilitating cross-frequency coupling (i.e., based on harmonic numerical ratios), as well as for facilitating controlled cross-frequency decoupling (i.e., based on non-harmonic numerical ratios approximating the golden mean 1.618…). In line with prior work (Rodriguez-Larios and Alaerts, 2019, 2020), the current study confirmed a proportionally high incidence of cross-frequency relationships approximating the non-harmonic 'decoupled' 1.6:1 cross-frequency state during resting-state, thereby providing further experimental support that this configuration forms a prevalent physiological state within the intrinsic EEG frequency architecture. Importantly, this study showed that, intranasal administration of OT, not PL induced a further facilitation of the formation of non-harmonic, decoupled ratio aspects (and a reduction of the formation of the harmonic 2:1 ratio aspect), predominantly due to a deceleration of peak alpha frequencies and an acceleration of peak theta frequencies.

To date, some initial EEG studies have yielded important insights into the effect of OT on temporal characteristics of neural processing, showing task-related changes in event-related potentials (de Bruijn et al., 2017; Peltola et al., 2018; Ruissen and de Bruijn, 2015; Waller et al., 2015; Ye et al., 2017) and band power (including e.g., the mu rhythm (Festante et al., 2020; Singh et al., 2016; Wynn et al., 2019) and frontal alpha asymmetry (Soriano et al., 2020)). One study by Schiller et al. (2019) examined the effect of a single-dose of OT versus PL on temporal characteristics of resting EEG networks, and showed OT administration to generally reduce the rapid switching among neural networks by increasing their temporal stability (Schiller et al., 2019). Another resting-state EEG study examined spectral changes in different frequency bands and showed no overall effect of OT on intrinsic band power activity of the alpha, theta, or delta and beta band, suggesting that OT does not induce a general change in neural activity following administration (Rutherford et al., 2018). Our findings corroborate these observations, indicating no overall changes in alpha or theta band power amplitude after OT administration.

Interestingly, the demonstrated OT-related changes in cross-frequency dynamics were shown to be paralleled by changes in ANS function, indicating a significant increase in high-frequency HRV - an established marker of parasympathetic nervous system (PNS) 'rest-and-digest' autonomic function - as well as a decrease in low-frequency HRV - influenced by a mix of vagal, sympathetic nervous system (SNS) activity, and baroreflex mechanisms (Shaffer et al., 2014). These observations are in line with four prior studies, showing an increase in resting-state high-frequency HRV after a single-dose of OT (Jain et al., 2017; Kemp et al., 2012; Martins et al., 2020; Norman et al., 2011). One study with chronic back pain patients showed no effect of OT on rest HRV, but here, small decreases in both high- and low-frequency HRV were noted during a mental arithmetic task, suggesting that OT differentially impacted HRV depending on whether the task context entailed a resting state or a state of (mild) cognitive stress (Tracy et al., 2018).

While this is the first study examining OT's role in modulating harmonicity of cross-frequency relationships, prior research has shown task-dependent shifts in harmonic/non-harmonic cross-frequency dynamics in the context of active cognitive processing and meditation (Rodriguez-Larios and Alaerts, 2019, 2020; Rodriguez-Larios et al., 2020a; Rodriguez-Larios et al., 2020b), indicating that meditative practice facilitated a preclusion of unwanted 'spurious' interactions among theta and alpha neural rhythms (increased non-harmonic cross-frequency ratio) (Rodriguez-Larios and Alaerts,

2020; Rodriguez-Larios et al., 2020b), whereas active cognitive processing states, as measured during a demanding arithmetic task, were associated with enhanced 'coupling' between alpha and theta rhythms, implicated in executive and memory processes (Rodriguez-Larios and Alaerts, 2019; Rodriguez-Larios et al., 2020a). Interestingly, several theoretical accounts (Colonnello et al., 2017; Ito et al., 2019; Mascaro et al., 2015) and also some initial empirical studies (Bellosta-Batalla et al., 2020a; Bellosta-Batalla et al., 2020b; Isgett et al., 2016; Lipschitz et al., 2015; Rockliff et al., 2011; Van Cappellen et al., 2016) have placed the oxytocinergic system at the center of mediating beneficial effects of meditation practice. For example, several studies showed that beneficial behavioral effects of mindfulness training were paralleled by higher endogenous production of OT post-intervention (Bellosta-Batalla et al., 2020a; Bellosta-Batalla et al., 2020b; Lipschitz et al., 2015). Also some initial OT administration studies showed a single-dose of OT to improve positive 'immersive' feelings during meditative practice (Van Cappellen et al., 2016) and the ease of developing compassionate qualities during compassion-focused meditation (Rockliff et al., 2011) (a component of mindfulness training). Together, it is tempting to speculate that the identified changes in cross-frequency harmonicity may form a common neural substrate by which meditative practice and acute OT administration facilitate homeostatic balance, i.e., by promoting a preclusion of unwanted 'spurious' interactions among neural rhythms during inactive rest.

The induction of high signal-to-noise states has been suggested to form a shared over-arching mechanism by which OT may amplify signal value of neuronal transmissions within wide-spread neural circuits (Maier et al., 2016; Oettl et al., 2016; Owen et al., 2013). At the brain's system level, OT may similarly promote high signal-to-noise states by efficiently reconfiguring neural networks into a 'resting state' neutral/decoupled state when no active task is at hand. Although indirect, OT's role in reducing the spontaneous occurrence of 'noisy' background couplings during an inactive resting state may therefore reconcile two prominent mechanistic theories of OT's effects, suggesting (i) a role of OT in top-down modulation of social salience, enhancing social sensitivity (Shamay-Tsoory and Abu-Akel, 2016), as well as (ii) a bottom-up function in regulating central and autonomic homeostatic function impacting (social) stress and anxiety responses (Stoop, 2012). In support of the latter, OT may facilitate increased autonomic homeostatic balance by facilitating the highest physiologically possible desynchronized state in the resting brain. The observation that baseline variations in HRV were associated with variations in non-harmonic cross-frequency arrangements is in support of this notion,

i.e., indicating that oscillatory systems with a low incidence of spurious, 'noisy' cross-frequency couplings are reflected by higher PNS drive. Also, in line with OT's purported role in modulating (social) salience, it can be hypothesized that OT may amplify signal value or attentional salience (e.g., of survival-relevant stimuli or stressors) by preventing noisy background couplings to interfere with efficient transitions to active signal processing states. In other words, OT can be suggested to act as a neuromodulatory filter, favouring the processing of survival-relevant information by dampening noisy background couplings. In this view, an efficient re-configuration into a neutral/ decoupled state during inactive rest - avoiding residual, spurious ('noisy') couplings - is suggested to form an important mechanism by which OT optimally prepares the system for forthcoming active signal processing states.

The following limitations and directions for future research are noted. While EEG allows a direct exploration of the temporal characteristics of neural activity, the precise anatomic origin of these neural oscillations are uncertain. OT-induced changes in non-harmonic cross-frequency decoupling were identified wide-spread across electrodes, whereas changes in cross-frequency harmonicity appeared to be more confined to particular fronto-temporal sites, suggesting differences in the spatial specificity of the observed effects. However, given the small number of electrodes, source localization could not be reliably performed in our data, and therefore, it would be interesting for future studies to address these relevant questions relating to the spatial distributions of OT's effects on cross-frequency dynamics further. Further, the inclusion of only young adult men in the current study is considered a limitation, rendering the generalizability of the observed effects across age and sex uncertain. Differential effects of OT depending on sex have been observed before, both at the behavioral and neural level, e.g. in terms of amygdala function (Wigton et al., 2015), emphasizing the need for future studies to explicitly model sex-dependent modulations of OT's effects. Finally, as highlighted above, the current observations of OT's modulatory effects on cross-frequency dynamics were observed during a low-stress, resting-state condition. Future research may be warranted to explore these dynamics within task-related contexts, e.g., allowing to draw links between (behavioural) changes in social salience/sensitivity and cross-frequency dynamics. This notion is important, considering that context and state-dependent changes are highlighted as important factors for inducing variations in OT's neuromodulatory effects (e.g. differential effects on rest (Jain et al., 2017; Kemp et al., 2012; Martins et al., 2020; Norman et al., 2011) versus task-related HRV (Tracy et al., 2018)). In this view, it

has been suggested that OT may primarily promote the restoration of autonomic balance (enhanced PNS drive) in the relative absence of acute stressors, but that opposite effects may be induced in task contexts that induce (mild) states of acute stress, in which case a facilitation of SNS-driven arousal and attentional salience may be evident (Carter, 2014). Further research is warranted to explore the role of (task-)context further in modulating OT's neurophysiologic effects.

Together, the current study showed neuromodulatory effects of OT on the harmonicity of alpha-theta cross-frequency interactions, indicative of a relative increase in non-harmonic 'decoupled' relationships between alpha and theta rhythms, as well as concurrent OT-induced enhancements in cardiac parasympathetic ANS drive (high-frequency HRV). In sum, the OT-induced increase in decoupling of theta and alpha rhythms - rendering them to operate more isolated from each other - is interpreted to reflect a role of OT in increasing the signal-to-noise ratio of the intrinsic EEG neural frequency architecture, namely, by reducing the occurrence of residual, 'noisy' couplings among neural rhythms facilitating a resting brain state.

Figure legends

Figure 1

Transient detection of alpha and theta peak frequencies and determination of cross-frequency relationships.

Transient peak frequencies of the theta (4–8 Hz) and alpha (8–14 Hz) bands were detected within 1 sec epochs and the numerical ratio between the alpha and theta peak frequencies was calculated ($peak\text{-}frequency_{alpha}/peak\text{-}frequency_{theta}$).

A. Visualization of the transient (epoch-wise) variability of alpha and theta peak frequencies over time (i.e., 10 sec) for an exemplary subject and electrode, as well as the transient numerical ratio over time.

B. Visualization of the frequency spectra of two exemplary epochs in which the identified alpha and theta peak frequencies (indicated by asterisks) formed a harmonic (2:1) versus a nonharmonic (1.6:1) cross-frequency relationship.

C. Visualization of the relative occurrence of all possible cross-frequency relationship (proportion of epochs, averaged across electrodes) as recorded at baseline (before nasal spray administration), showing a maximal occurrence of the non-harmonic 1.6:1 alpha:theta ratio aspect (10.16%, average across electrodes). The harmonic 2:1 ratio aspect showed an average occurrence of 7.76% (across electrodes). Visualizations are partly adapted from (Rodriguez-Larios and Alaerts, 2019)).

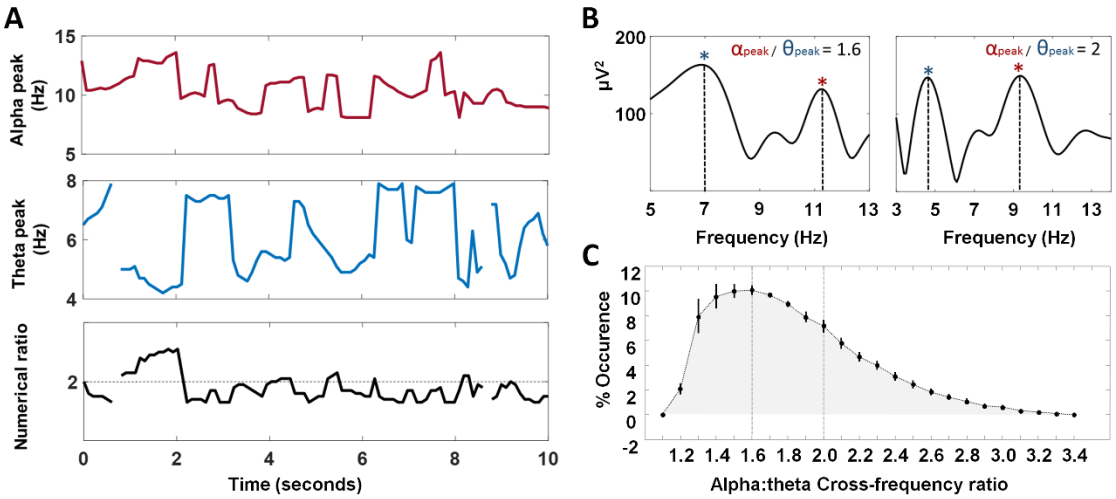

Figure 2

Assessment of treatment-related differences in the occurrence of 1.6:1 and 2:1 alpha:theta cross-frequency ratios.

Box plots visualize mean pre-to-post changes in the occurrence of the 1.6:1 and 2:1 ratio aspect (averaged across all electrodes), separately for the oxytocin and placebo group (including standard error (SE) and 1.96 SE). The relative pre-to-post increase in the 1.6:1 ratio aspect and the relative pre-to-post decrease in the 2:1 ratio aspect were significantly more pronounced in the oxytocin group compared to the placebo group.

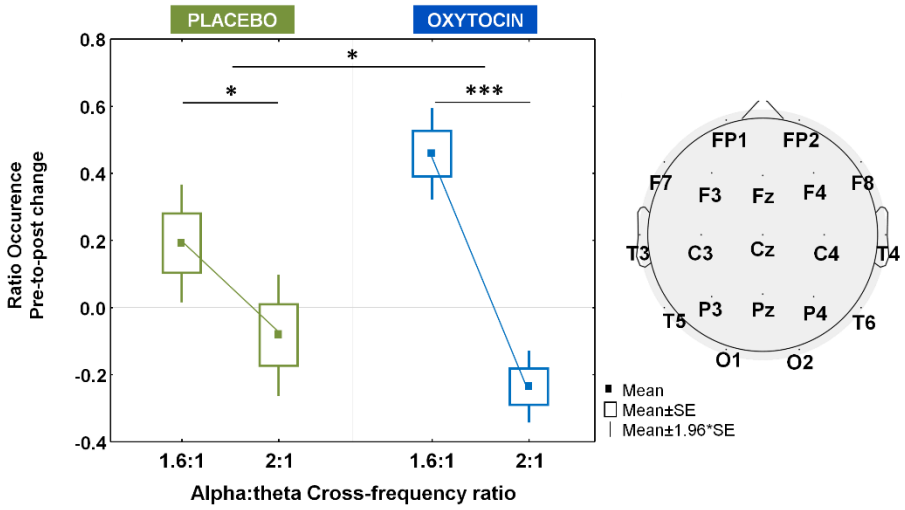

Figure 3

Treatment-related differences in the occurrence of 1.6:1 non-harmonic decoupling.

A. Pre-to-post changes in the occurrence of the 1.6:1 non-harmonic ratio aspect, visualized separately for the oxytocin (top) and placebo (lower panel) group. In the oxytocin group, a large cluster of electrodes, spanning electrodes Fp1, Fp2, F7, F3, Fz, F4, T3, C3, C4, T4, T5, Pz, P4, T6 was identified, showing significant pre-to-post increases in the 1.6:1 ratio occurrence. Topographical heat maps represent t-values (single-sample t-tests) at each electrode with asterisks marking significant electrodes ($p_{FDR} < .05$). Vertical bars denote +/- standard errors (SE).

B. Cluster-level analysis confirmed a treatment-specific increase in the occurrence of the 1.6:1 non-harmonic ratio in the oxytocin group, not in the placebo group. Box plots visualize mean pre-to-post changes in 1.6:1 ratio occurrences (including SE and 1.96 SE), averaged across depicted cluster electrodes Fp1, Fp2, F7, F3, Fz, F4, T3, C3, C4, T4, T5, Pz, P4, T6.

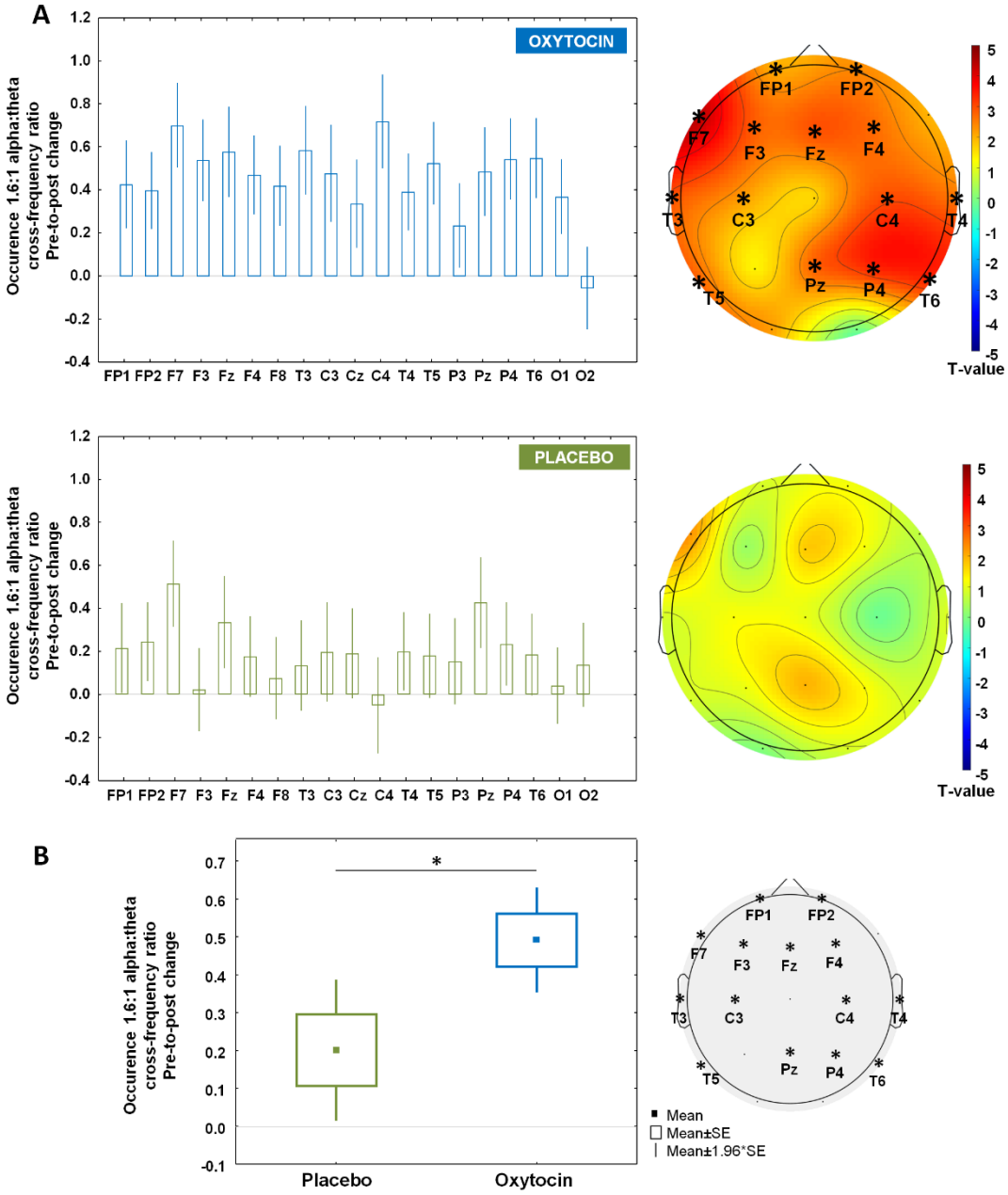
A
OXYTOCIN
Occurence 1.6:1 alpha:theta
cross-frequency ratio
Pre-to-post change
1.2
1.0
0.8
0.6
0.4
0.2
0.0
-0.2
-0.4
FP1 FP2 F7 F3 Fz F4 F8 T3 C3 Cz C4 T4 T5 P3 Pz P4 T6 O1 O2
FP1
FP2
F7
F3
Fz
F4
T3
C3
C4
T4
Pz
P4
T5
T6
5
4
3
2
1
0
-1
-2
-3
-4
-5
T-value
PLACEBO
Occurence 1.6:1 alpha:theta
cross-frequency ratio
Pre-to-post change
1.2
1.0
0.8
0.6
0.4
0.2
0.0
-0.2
-0.4
FP1 FP2 F7 F3 Fz F4 F8 T3 C3 Cz C4 T4 T5 P3 Pz P4 T6 O1 O2
5
4
3
2
1
0
-1
-2
-3
-4
-5
T-value
B
Occurence 1.6:1 alpha:theta
cross-frequency ratio
Pre-to-post change
0.7
0.6
0.5
0.4
0.3
0.2
0.1
0.0
-0.1
*
Placebo
Oxytocin
FP1
FP2
F7
F3
Fz
F4
T3
C3
C4
T4
Pz
P4
T5
T6
Mean
Mean±SE
Mean±1.96*SE

Figure 4

Treatment-related differences in the occurrence of 2:1 harmonic coupling.

A. Pre-to-post changes in the occurrence of the 2:1 harmonic ratio aspect, visualized separately for the oxytocin (top) and placebo (lower panel) group. In the oxytocin group, a subset of electrodes, spanning electrodes F7, F3, F4, T5, Pz, T6 was identified, showing significant pre-to-post decreases in the 2:1 ratio occurrence. Topographical heat maps represent t-values (single-sample t-tests) at each electrode with asterisks marking significant electrodes ($p_{FDR} < .05$). Vertical bars denote +/- standard errors (SE).

B. Cluster-level analysis confirmed a treatment-specific decrease in the occurrence of the 2:1 non-harmonic ratio in the oxytocin group, not in the placebo group. Box plots visualize mean pre-to-post changes in 2:1 ratio occurrences (including SE and 1.96 SE), averaged across depicted cluster electrodes F7, F3, F4, T5, Pz, T6.

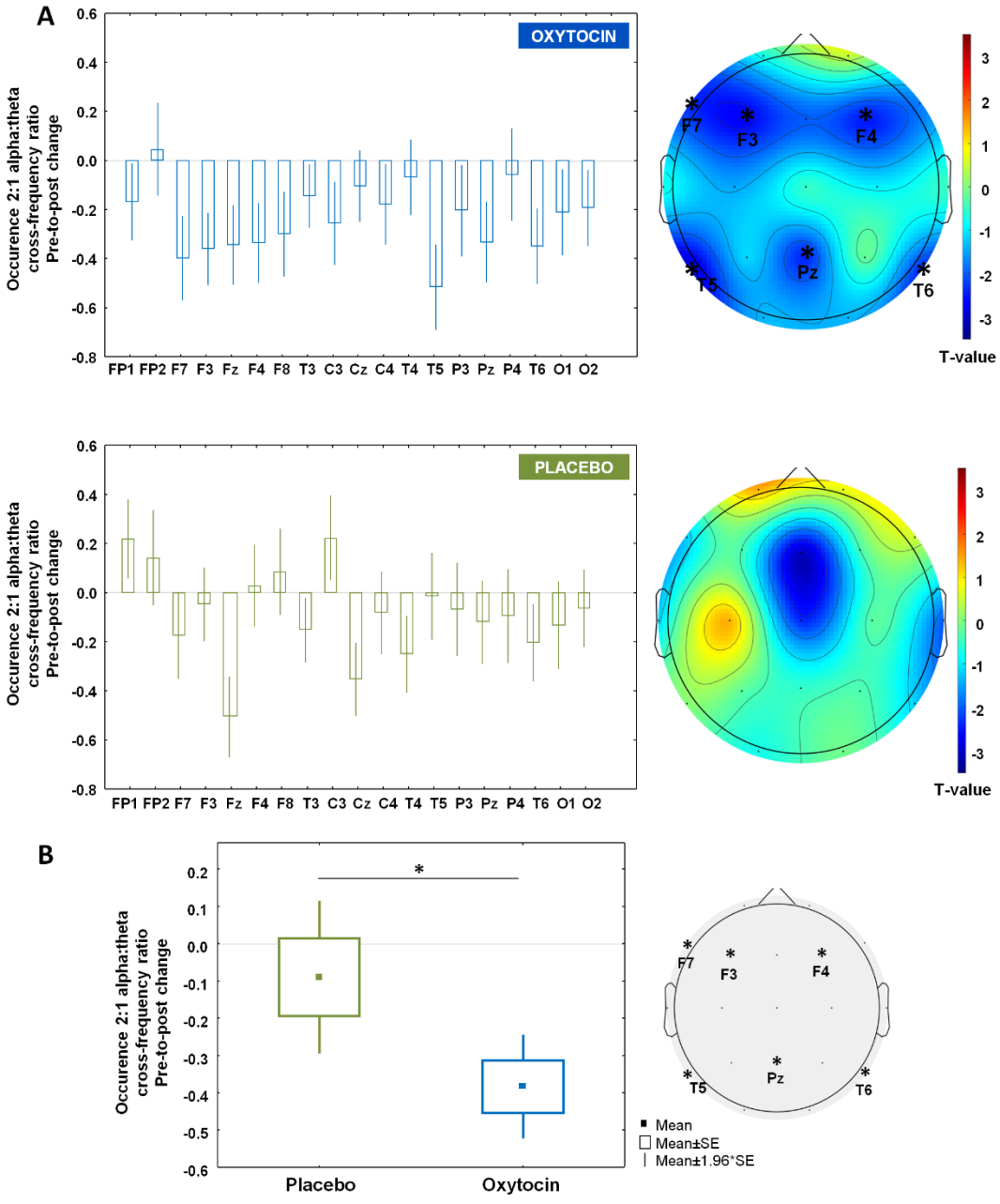
A
OXYTOCIN
Occurence 2:1 alpha:theta
cross-frequency ratio
Pre-to-post change
0.6
0.4
0.2
0.0
-0.2
-0.4
-0.6
-0.8
FP1 FP2 F7 F3 Fz F4 F8 T3 C3 Cz C4 T4 T5 P3 Pz P4 T6 O1 O2
F7
F3
F4
Pz
T5
T6
3
2
1
0
-1
-2
-3
T-value
PLACEBO
Occurence 2:1 alpha:theta
cross-frequency ratio
Pre-to-post change
0.6
0.4
0.2
0.0
-0.2
-0.4
-0.6
-0.8
FP1 FP2 F7 F3 Fz F4 F8 T3 C3 Cz C4 T4 T5 P3 Pz P4 T6 O1 O2
3
2
1
0
-1
-2
-3
T-value
B
Occurence 2:1 alpha:theta
cross-frequency ratio
Pre-to-post change
0.2
0.1
0.0
-0.1
-0.2
-0.3
-0.4
-0.5
-0.6
*
Placebo
Oxytocin
F7
F3
F4
Pz
T5
T6
Mean
Mean±SE
Mean±1.96*SE

Figure 5

Assessment of treatment-related changes in heart rate variability.

A. Pre-to-post changes in high-frequency and low-frequency heart rate variability (HRV), visualized separately for the oxytocin and placebo group. Vertical bars denote +/- standard errors (SE).

B. Visualization of the relationship between baseline recorded (before nasal spray) HRV and the occurrence of the non-harmonic 1.6:1 ratio aspect (averaged across depicted cluster electrodes Fp1, Fp2, F7, F3, Fz, F4, T3, C3, C4, T4, T5, Pz, P4, T6). Grey lines denote 95% confidence bands.

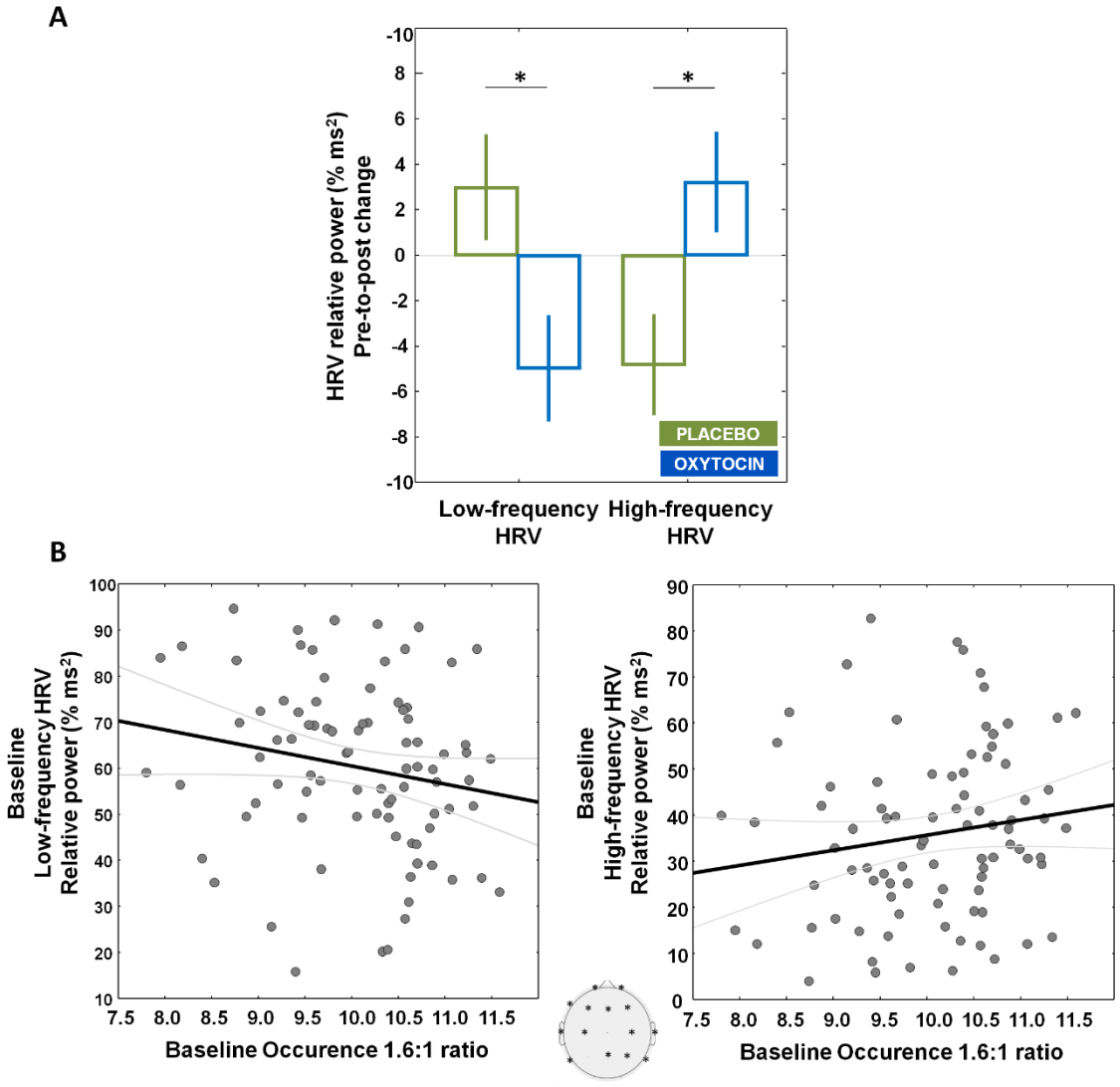

Author Disclosures

Acknowledgements. The authors would like to thank Elisa Maes, Julio Rodriguez Larios and Marie Quartier for their contribution in the data collection and processing, as well as to all students and participants collaborating in this study.

Contributions. Authors KA, ND and JP designed the study and KA wrote the first draft of the manuscript. Author KA and ND managed the literature searches and statistical analyses. Author AT, ND and JP managed the data collection. All authors contributed to and have approved the final manuscript.

Funding. Funding for this study was provided by grants from the Flanders Fund for Scientific Research (FWO G079017N and G046321N) and the Branco Weiss fellowship of the Society in Science - ETH Zurich granted to KA. ND is supported by an internal C1 fund of the KU Leuven [ELG-D2857-C14/17/102]. JP is supported by the Marguerite-Marie Delacroix foundation and a postdoctoral fellowship of the Flanders Fund for Scientific Research (FWO 1257621N). The funding sources had no further role in study design, data collection, analysis and interpretation of data, writing of the report or in the decision to submit the paper for publication.

Competing interests. The authors report no competing interests.

References

Bartz, J.A., Zaki, J., Bolger, N., Ochsner, K.N., 2011. Social effects of oxytocin in humans: context and person matter. Trends Cogn Sci 15, 301-309.

Bellosta-Batalla, M., Blanco-Gandía, M.C., Rodríguez-Arias, M., Cebolla, A., Pérez-Blasco, J., Moya-Albiol, L., 2020a. Increased Salivary Oxytocin and Empathy in Students of Clinical and Health Psychology After a Mindfulness and Compassion-Based Intervention. Mindfulness 11, 1006-1017.

Bellosta-Batalla, M., Del Carmen Blanco-Gandía, M., Rodríguez-Arias, M., Cebolla, A., Pérez-Blasco, J., Moya-Albiol, L., 2020b. Brief mindfulness session improves mood and increases salivary oxytocin in psychology students. Stress Health 36, 469-477.

Carter, C.S., 2014. Oxytocin pathways and the evolution of human behavior. Annu Rev Psychol 65, 17-39.

Colonnello, V., Petrocchi, N., Farinelli, M., Ottaviani, C., 2017. Positive Social Interactions in a Lifespan Perspective with a Focus on Opioidergic and Oxytocinergic Systems: Implications for Neuroprotection. Curr Neuropharmacol 15, 543-561.

Daniels, N., Prinsen, J., Soriano, J.R., Alaerts, K., 2020. Oxytocin enhances the recovery of eye-contact induced autonomic arousal: A treatment mechanism study with placebo-controlled design. European Neuropsychopharmacology 000, 1-12.

de Bruijn, E.R.A., Ruissen, M.I., Radke, S., 2017. Electrophysiological correlates of oxytocin-induced enhancement of social performance monitoring. Soc Cogn Affect Neurosci 12, 1668-1677.

Festante, F., Ferrari, P.F., Thorpe, S.G., Buchanan, R.W., Fox, N.A., 2020. Intranasal oxytocin enhances EEG mu rhythm desynchronization during execution and observation of social action: An exploratory study. Psychoneuroendocrinology 111, 104467.

Fries, P., 2005. A mechanism for cognitive dynamics: neuronal communication through neuronal coherence. Trends Cogn Sci 9, 474-480.

Georgiou, K., Larentzakis, A.V., Khamis, N.N., Alsuhaibani, G.I., Alaska, Y.A., Giallafos, E.J., 2018. Can Wearable Devices Accurately Measure Heart Rate Variability? A Systematic Review. Folia Med (Plovdiv) 60, 7-20.

Guastella, A.J., Hickie, I.B., McGuinness, M.M., Otis, M., Woods, E.A., Disinger, H.M., Chan, H.K., Chen, T.F., Banati, R.B., 2013. Recommendations for the standardisation of oxytocin nasal administration and guidelines for its reporting in human research. Psychoneuroendocrinology 38, 612-625.

Guastella, A.J., MacLeod, C., 2012. A critical review of the influence of oxytocin nasal spray on social cognition in humans: evidence and future directions. Horm. Behav 61, 410-418.

Isgett, S.F., Algoe, S.B., Boulton, A.J., Way, B.M., Fredrickson, B.L., 2016. Common variant in OXTR predicts growth in positive emotions from loving-kindness training. Psychoneuroendocrinology 73, 244-251.

Ito, E., Shima, R., Yoshioka, T., 2019. A novel role of oxytocin: Oxytocin-induced well-being in humans. Biophys Physicobiol 16, 132-139.

Jain, V., Marbach, J., Kimbro, S., Andrade, D.C., Jain, A., Capozzi, E., Mele, K., Del, R.R., Kay, M.W., Mendelowitz, D., 2017. Benefits of oxytocin administration in obstructive sleep apnea. Am. J. Physiol Lung Cell Mol. Physiol 313, L825-L833.

Kemp, A.H., Quintana, D.S., Kuhnert, R.L., Griffiths, K., Hickie, I.B., Guastella, A.J., 2012. Oxytocin increases heart rate variability in humans at rest: implications for social approach-related motivation and capacity for social engagement. PLoS One 7, e44014.

Klimesch, W., 2012. α-band oscillations, attention, and controlled access to stored information. Trends Cogn Sci 16, 606-617.

Klimesch, W., 2013. An algorithm for the EEG frequency architecture of consciousness and brain body coupling. Front Hum. Neurosci 7, 766.

Klimesch, W., 2018. The frequency architecture of brain and brain body oscillations: an analysis. Eur J Neurosci 48, 2431-2453.

Lipschitz, D.L., Kuhn, R., Kinney, A.Y., Grewen, K., Donaldson, G.W., Nakamura, Y., 2015. An Exploratory Study of the Effects of Mind-Body Interventions Targeting Sleep on Salivary Oxytocin Levels in Cancer Survivors. Integr Cancer Ther 14, 366-380.

Maier, P., Kaiser, M.E., Grinevich, V., Draguhn, A., Both, M., 2016. Differential effects of oxytocin on mouse hippocampal oscillations in vitro. Eur J Neurosci 44, 2885-2898.

Martins, D., Davies, C., De Micheli, A., Oliver, D., Krawczun-Rygmaczewska, A., Fusar-Poli, P., Paloyelis, Y., 2020. Intranasal oxytocin increases heart-rate variability in men at clinical high risk for psychosis: a proof-of-concept study. Transl Psychiatry 10, 227.

Mascaro, J.S., Darcher, A., Negi, L.T., Raison, C.L., 2015. The neural mediators of kindness-based meditation: a theoretical model. Front Psychol 6, 109.

Norman, G.J., Cacioppo, J.T., Morris, J.S., Malarkey, W.B., Berntson, G.G., Devries, A.C., 2011. Oxytocin increases autonomic cardiac control: moderation by loneliness. Biol. Psychol 86, 174-180.

Oettl, L.L., Ravi, N., Schneider, M., Scheller, M.F., Schneider, P., Mitre, M., da Silva, G.M., Froemke, R.C., Chao, M.V., Young, W.S., Meyer-Lindenberg, A., Grinevich, V., Shusterman, R., Kelsch, W., 2016. Oxytocin Enhances Social Recognition by Modulating Cortical Control of Early Olfactory Processing. Neuron 90, 609-621.

Owen, S.F., Tuncdemir, S.N., Bader, P.L., Tirko, N.N., Fishell, G., Tsien, R.W., 2013. Oxytocin enhances hippocampal spike transmission by modulating fast-spiking interneurons. Nature 500, 458-462.

Peltola, M.J., Strathearn, L., Puura, K., 2018. Oxytocin promotes face-sensitive neural responses to infant and adult faces in mothers. Psychoneuroendocrinology 91, 261-270.

Pletzer, B., Kerschbaum, H., Klimesch, W., 2010. When frequencies never synchronize: the golden mean and the resting EEG. Brain Res 1335, 91-102.

Rassi, E., Dorffner, G., Gruber, W., Schabus, M., Klimesch, W., 2019. Coupling and Decoupling between Brain and Body Oscillations. Neuroscience Letters 711, 134401-134401.

Rockliff, H., Karl, A., McEwan, K., Gilbert, J., Matos, M., Gilbert, P., 2011. Effects of intranasal oxytocin on 'compassion focused imagery'. Emotion 11, 1388-1396.

Rodriguez-Larios, J., Alaerts, K., 2019. Tracking Transient Changes in the Neural Frequency Architecture: Harmonic Relationships between Theta and Alpha Peaks Facilitate Cognitive Performance. J Neurosci 39, 6291-6298.

Rodriguez-Larios, J., Alaerts, K., 2020. EEG alpha-theta dynamics during mind wandering in the context of breath focus meditation: an experience sampling approach with novice meditation practitioners. Eur J Neurosci.

Rodriguez-Larios, J., Faber, P., Achermann, P., Tei, S., Alaerts, K., 2020a. From thoughtless awareness to effortful cognition: alpha - theta cross-frequency dynamics in experienced meditators during meditation, rest and arithmetic. Sci Rep 10, 5419.

Rodriguez-Larios, J., Wong, K.F., Lim, J., Alaerts, K., 2020b. Mindfulness Training is Associated with Changes in Alpha-Theta Cross-Frequency Dynamics During Meditation. Mindfulness 11, 2695-2704.

Roopun, A.K., Kramer, M.A., Carracedo, L.M., Kaiser, M., Davies, C.H., Traub, R.D., Kopell, N.J., Whittington, M.A., 2008. Temporal Interactions between Cortical Rhythms. Front Neurosci 2, 145-154.

Ruissen, M.I., de Bruijn, E.R., 2015. Is it me or is it you? Behavioral and electrophysiological effects of oxytocin administration on self-other integration during joint task performance. Cortex 70, 146-154.

Rutherford, H.J.V., Guo, X.M., Wu, J., Graber, K.M., Hayes, N.J., Pelphrey, K.A., Mayes, L.C., 2018. Intranasal oxytocin decreases cross-frequency coupling of neural oscillations at rest. Int J Psychophysiol 123, 143-151.

Sauseng, P., Klimesch, W., Gruber, W.R., Birbaumer, N., 2008. Cross-frequency phase synchronization: a brain mechanism of memory matching and attention. Neuroimage 40, 308-317.

Schäfer, A., Vagedes, J., 2013. How accurate is pulse rate variability as an estimate of heart rate variability? A review on studies comparing photoplethysmographic technology with an electrocardiogram. Int J Cardiol 166, 15-29.

Schiller, B., Koenig, T., Heinrichs, M., 2019. Oxytocin modulates the temporal dynamics of resting EEG networks. Sci Rep 9, 13418.

Shaffer, F., McCraty, R., Zerr, C.L., 2014. A healthy heart is not a metronome: an integrative review of the heart's anatomy and heart rate variability. Frontiers in Psychology 5.

Shamay-Tsoory, S.G., Abu-Akel, A., 2016. The Social Salience Hypothesis of Oxytocin. Biol. Psychiatry 79, 194-202.

Singh, F., Nunag, J., Muldoon, G., Cadenhead, K.S., Pineda, J.A., Feifel, D., 2016. Effects of intranasal oxytocin on neural processing within a socially relevant neural circuit. Eur Neuropsychopharmacol 26, 626-630.

Soriano, J., Daniels, N., Prinsen, J., Alaerts, K., 2020. Intranasal oxytocin enhances approach-related EEG frontal alpha asymmetry during engagement of direct eye contact. Brain Communications.

Stoop, R., 2012. Neuromodulation by oxytocin and vasopressin. Neuron 76, 142-159.

Tarvainen, M.P., Niskanen, J.P., Lipponen, J.A., Ranta-Aho, P.O., Karjalainen, P.A., 2014. Kubios HRV--heart rate variability analysis software. Comput Methods Programs Biomed 113, 210-220.

Tracy, L.M., Gibson, S.J., Labuschagne, I., Georgiou-Karistianis, N., Giummarra, M.J., 2018. Intranasal oxytocin reduces heart rate variability during a mental arithmetic task: A randomised, double-blind, placebo-controlled cross-over study. Prog Neuropsychopharmacol Biol Psychiatry 81, 408-415.

Van Cappellen, P., Way, B.M., Isgett, S.F., Fredrickson, B.L., 2016. Effects of oxytocin administration on spirituality and emotional responses to meditation. Soc Cogn Affect Neurosci 11, 1579-1587.

Varela, F., Lachaux, J.P., Rodriguez, E., Martinerie, J., 2001. The brainweb: phase synchronization and large-scale integration. Nat. Rev. Neurosci 2, 229-239.

Waller, C., Wittfoth, M., Fritzsche, K., Timm, L., Wittfoth-Schardt, D., Rottler, E., Heinrichs, M., Buchheim, A., Kiefer, M., Gündel, H., 2015. Attachment representation modulates oxytocin effects on the processing of own-child faces in fathers. Psychoneuroendocrinology 62, 27-35.

Wigton, R., Radua, J., Allen, P., Averbeck, B., Meyer-Lindenberg, A., McGuire, P., Shergill, S.S., Fusar-Poli, P., 2015. Neurophysiological effects of acute oxytocin administration: systematic review and meta-analysis of placebo-controlled imaging studies. J. Psychiatry Neurosci 40, E1-22.

Wynn, J.K., Green, M.F., Hellemann, G., Reavis, E.A., Marder, S.R., 2019. A dose-finding study of oxytocin using neurophysiological measures of social processing. Neuropsychopharmacology 44, 289-294.

Ye, Z., Stolk, A., Toni, I., Hagoort, P., 2017. Oxytocin Modulates Semantic Integration in Speech Comprehension. J Cogn Neurosci 29, 267-276.

Tracking transient changes in the intrinsic neural frequency architecture: Oxytocin facilitates non-harmonic relationships between alpha and theta rhythms in the resting brain

Kaat Alaerts, Aymara Taillieu, Jellina Prinsen, Nicky Daniels

Supplementary Material

Supplementary Methods

To examine whether the reported treatment-related changes in 1.6:1 non-harmonic decoupling and 2:1 harmonic coupling were specific to these frequency arrangements, pre-to-post changes in the proportion of epochs displaying any of the other possible cross-frequency relationships (within a range of 1.2–2.5, step size 0.1) were computed and subjected to nonparametric cluster-based permutation statistics, identifying clusters that show significant OT versus PL treatment effects based on spatial (electrodes) and cross-frequency ratio adjacency (1000 permutations, $p < .05$ corrected for multiple comparisons, one-sided) (MATLAB toolbox FieldTrip (Maris and Oostenveld, 2007)). Note that, due to the absence of data for ratios smaller than 1.2 and greater than 2.5 (**Figure 1C**, less than 2 % occurrence), the analysis was performed for ratios within a range of 1.2 - 2.5 (step-size of 0.1).

Supplementary Results

A significant positive cluster overlapping non-harmonic ratio aspect 1.6:1 was identified, ranging between 1.3 and 1.7 (cluster $t(94) = 55.98$; $p_{corrected} = 0.05$), indicating an increase in the incidence of these low-range cross-frequency ratios in the OT, compared to the PL group. At trend-level, also a negative cluster overlapping harmonic ratio aspect 2:1 was identified, ranging from ratio 1.8-2.5, but the effect failed to reach significance at the applied cluster threshold (cluster $t(94) = 44.28$; $p_{corrected} = 0.088$). The spatial distribution of these clusters is visualized in **Supplementary Figure 1**. In sum, these exploratory analyses showed that a single-dose of OT induced an increase in a set of lower-end ratios centered around 1.6:1 (i.e., ranging from 1.3 - 1.7), and - at trend-level - a relative decrease in the occurrence of cross-frequency ratios overlapping harmonic ratio 2:1 (i.e., 1.8 - 2.5).

Supplementary Figure 1

Assessment of treatment-related differences in the occurrence of different alpha:theta cross-frequency relationships.

The scaled color plot visualizes the respective independent samples t-test values (oxytocin (OT) versus placebo (PL)) separately for each electrode (y-axis) and cross-frequency ratio (x-axis). Warm colors indicate electrodes showing a relative pre-to-post increase in ratio occurrence in the OT, compared to the PL group. Blue colors indicate electrodes showing a relative pre-to-post decrease in ratio occurrence in the OT, compared to the PL group.

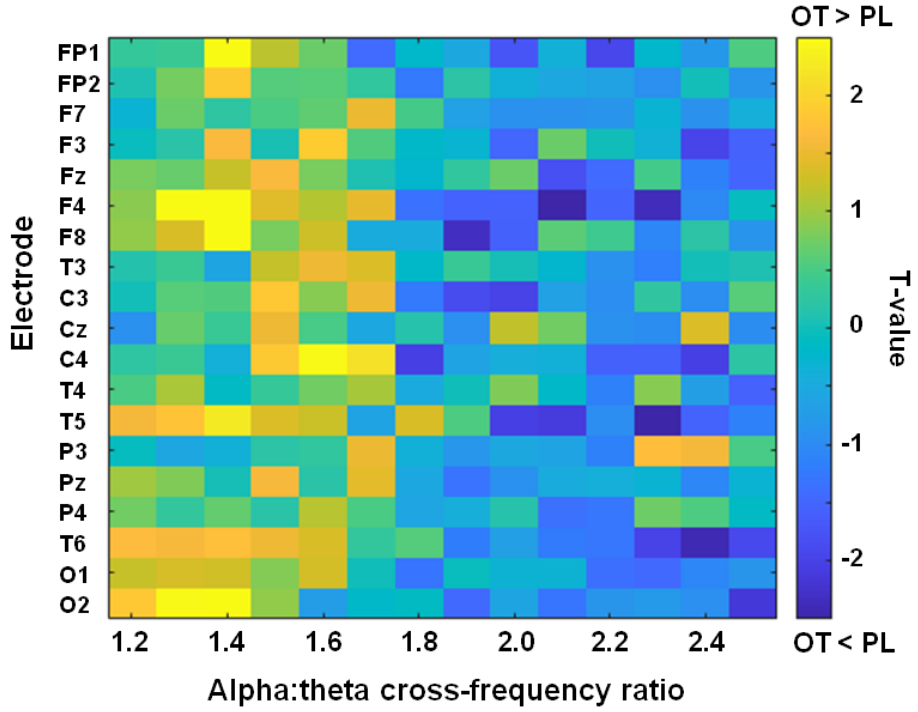

References

Maris, E., Oostenveld, R., 2007. Nonparametric statistical testing of EEG-and MEG-data. Journal of Neuroscience Methods 164, 177-190.